

# **New data on Cu-exchanged phillipsite: a multi-methodological study**

**Running title:** Cu-exchanged phillipsite

**Abstract**

**Introduction**

**Materials and experimental methods**

**-Mineralogy**

**-Experimental methods**

**Results and discussion**

**Acknowledgements**

**References**

**Tables/Figure captions**

**Corresponding author: G. Diego Gatta**

Dipartimento Scienze della Terra

Università degli Studi di Milano

Via Botticelli, 23

I-20133 Milano, Italy

Tel. +39 02 503 15607

Fax +39 02 503 15597

E-Mail: [diego.gatta@unimi.it](mailto:diego.gatta@unimi.it)

*Manuscript submitted to Physics and Chemistry of Minerals*

# New data on Cu-exchanged phillipsite: a multi-methodological study

G. Diego Gatta<sup>1,2</sup>, Piergiulio Cappelletti<sup>3</sup>, Bruno de' Gennaro<sup>4</sup>, Nicola Rotiroli<sup>1</sup>, Alessio Langella<sup>5</sup>

<sup>1</sup>Dipartimento di Scienze della Terra, Università degli Studi di Milano,

Via Botticelli 23, I-20133 Milano, Italy

<sup>2</sup>CNR - IC, Sede di Bari, Via G. Amendola 122/o, Bari, Italy

<sup>3</sup>Dipartimento di Scienze della Terra, dell'Ambiente e delle Risorse, Università degli Studi di

Napoli Federico II, Via Mezzocannone 8, I-80134, Napoli, Italy

<sup>4</sup>Dipartimento di Ingegneria Chimica, dei Materiali e della Produzione industriale, Università degli

Studi di Napoli Federico II, P.le Tecchio 80, I-80125 Napoli

<sup>5</sup>Dipartimento di Studi Geologici e Ambientali, Università degli Studi del Sannio, Via dei Mulini

59/A, I-82100, Benevento, Italy

Corresponding author: [diego.gatta@unimi.it](mailto:diego.gatta@unimi.it)

## Abstract

The cation exchange capacity of a natural phillipsite-rich sample from the Neapolitan Yellow Tuff, Southern Italy (treated in order to obtain a 95 wt. % zeolite-rich sample composed mainly of phillipsite and minor chabazite) for Cu was evaluated using the batch exchange method. The sample had previously been exchanged into its monocationic form (Na), and then used for the equilibrium studies of the exchange reaction  $2\text{Na}^+ \rightleftharpoons \text{Cu}^{2+}$ . Reversibility ion exchange tests were performed. The isotherm displays an evident hysteresis loop. Interestingly, the final Cu-exchanged polycrystalline material was green-bluish. Natural, Na- and Cu-exchanged forms were analyzed by X-ray powder diffraction, and the Cu-phillipsite was also investigated by transmission electron microscopy (TEM). Structure refinement of Cu-phillipsite was performed by the Rietveld method using synchrotron data, and it indicates a small, but significant, fraction of Cu sharing with Na two-three independent extra-framework sites. The TEM experiment shows sub-spherical nano-clusters of crystalline species (with average size of 5 nm) lying on the surfaces of zeolite crystals or dispersed

in the amorphous fraction, with electron diffraction patterns corresponding to those of CuO (tenorite-like structure) and Cu(OH)<sub>2</sub> (spertiniite-like structure). X-ray and TEM investigations show that Cu is mainly concentrated in different species (crystalline or amorphous) within the sample, not only in phillipsite. The experimental findings based on X-ray and TEM investigations, along with the hysteresis loop of the ion exchange tests, are discussed and some general considerations about the mechanisms of exchange reactions involving divalent cations with high hydration energy are provided.

**Keywords:** Zeolite; phillipsite; Cu-exchange capacity; Rietveld structure refinement; TEM investigation.

## Introduction

Phillipsite, one of the most common natural zeolites, is generally found in vugs of massive volcanic rocks, in basalts and tuffs as an alteration product of glass, or in sediments altered by diagenesis in “closed and/or open hydrologic systems” (Galli et al. 1972; Gottardi and Galli 1985; Langella et al. 2001; Passaglia and Sheppard 2001; Sheppard et al. 2001; Gatta et al. 2009). Phillipsite crystals (ideal composition  $K_2(Na,Ca_{0.5})_3[Al_5Si_{11}O_{32}] \cdot 12H_2O$ ) (Passaglia and Sheppard 2001; Coombs et al. 1997) usually occur in spherical radial aggregates and are ubiquitously twinned (Černý 1964; Rinaldi et al. 1974) and intergrown with several other zeolites (*e.g.* faujasite, offretite, gismondine, garronite and gobbinsite) (Passaglia and Sheppard 2001; Rinaldi et al. 1975).

The crystal structure of phillipsite was solved by Rinaldi et al. (1974) on the basis of single-crystal X-ray diffraction data, and recently re-investigated by Gatta et al. (2009). The symmetry of natural phillipsite is monoclinic, with space group  $P2_1/m$ , with  $a \sim 9.865$ ,  $b \sim 14.300$ ,  $c \sim 8.693$  Å and  $\beta \sim 124.81^\circ$ . Wide ranges of Si/(Si+Al), K/(K+Ba) and Na/(Na+Ca) ratios have been reported for natural phillipsites (Alberti 1978; Passaglia and Sheppard 2001; Gatta et al. 2009). Actually, the

wide variation in the extra-framework population reflects the chemical composition of the precursor reacting glass, as well as the chemical composition of the fluids interacting with the precursor, or post-formational exchange processes (de' Gennaro et al. 1982, 1999). A recent study has provided new insights into the crystal-chemistry of phillipsites collected in different outcrops from one of the largest volcanoclastic deposits of the Mediterranean area, the Neapolitan Yellow Tuff (NYT, Southern Italy) (Gatta et al. 2010). One of the main results reported by Gatta et al. (2010) was significantly different populations of extra-framework cations (*i.e.*, K, Na and Ca) and H<sub>2</sub>O molecules observed in crystals from different localities. A small but significant control of the crystal-chemistry on the unit-cell parameters was also observed (Gatta et al. 2010).

A solid knowledge of the crystal-chemistry of phillipsites from the NYT and the search for an efficient and inexpensive sequestering agents for heavy metals, led us to extend our investigation to this naturally-occurring and low-cost microporous material, exploring its cationic exchange capacity with Cu. Among zeolites, phillipsite is considered a microporous compound with a significant affinity for Cu (Ming and Mumpton 1995; Tsitsishvili et al. 1992; Colella et al. 1998). However, earlier studies reported only indirect evidence for the sequestration ability of this zeolite for Cu, whereas structural characterizations of Cs<sup>+</sup>-, NH<sub>4</sub><sup>+</sup>-, Sr<sup>2+</sup>- and Ba<sup>2+</sup>-exchanged phillipsite were successfully performed by Rietveld method by Gualtieri (2000) and Gualtieri et al. (1999a, 1999b, 2000). In this light, the aim of this study is to provide direct evidence of the sequestration ability of phillipsite for Cu by investigating the mechanisms on the atomic scale with a multi-methodological approach.

## **Materials and experimental methods**

### **- Mineralogy**

The sample used for the present investigation comes from an outcrop of NYT within the caldera of Campi Flegrei, namely Grotta del Sole locality, and labelled "P7" in Figure 1. The Neapolitan Yellow Tuff (15,000 years BP) (Insinga et al. 2006), is the product of a powerful

phreatomagmatic eruption of Campi Flegrei volcanic district (Southern Italy) and occurs as a thick and widespread pyroclastic deposit on the periphery of Campi Flegrei, within the city of Napoli and in the Campanian Plain. The setup of favourable physical-chemical conditions soon after the emplacement of this pyroclastite led to the crystallization of zeolites, mainly phillipsite and subordinate chabazite and analcime (de' Gennaro et al. 2000). The chemical composition of phillipsites from NYT was reported in previous studies by various authors (Passaglia 1985; de' Gennaro et al. 1990; Gatta et al. 2010).

The starting material used in this multi-methodological study was collected on an abandoned quarry front, which favoured the sampling at different stratigraphic heights. This was necessary in order to obtain a homogeneous and representative sample of the outcrop. After the removal of all traces of surface alterations, the samples were ground and sieved. The 60-125 mesh grain-size fraction was selected for further enrichment operations as it turned to be the richest in zeolites. A combination of ultrasonic bath, centrifugation and a final magnetic separation (Frantz isodynamic separator) resulted in a 95 wt% zeolite-rich sample composed of dominant phillipsite and minor chabazite. Phillipsite mostly occurs as clusters of needle-shaped crystals ranging from a few to several tens of microns in size.

#### **- Experimental methods**

X-ray powder diffraction data (XRPD) of the investigated samples were collected with an automated *Panalytical X'Pert Pro* modular diffractometer equipped with a RTMS fast detector *X'Celerator*. Operating conditions were: monochromatic  $\text{CuK}\alpha$  radiation, 40 kV, 40 mA,  $2\theta$ -range from 4 to  $100^\circ$ , step size of  $2\theta = 0.017^\circ$ , counting time of 240 s per step. Powders with grain size <10 microns were obtained by means of a McCrone micronising mill (agate cylinders and wet grinding time 15 min). To minimize preferred orientations, the sample was carefully side-loaded onto an aluminium sample holder with an oriented quartz mono-crystal underneath. The diffraction patterns were successfully indexed on the monoclinic unit-cell previously reported by Rinaldi et al.

(1974) and Gatta et al. (2009) (*i.e.*,  $a \sim 9.92$ ,  $b \sim 14.31$ ,  $c \sim 8.74$  Å,  $\beta \sim 124.9^\circ$ ), and the reflection conditions are consistent with the space group  $P2_1/m$ . The Rietveld structure refinement (Rietveld 1969) was then performed. Further details pertaining to the refinement protocol, atomic positions, thermal displacement parameters and bond distances of the natural phillipsite “P7”, used for the present study, are reported in Gatta et al. (2010). The sample “P7” was selected as the most suitable due to its high Na content (Table 1 in Gatta et al. 2010), since the exchange process was aimed at obtaining a monocationic Na-form.

Cation exchange capacity (CEC) of the phillipsite sample was evaluated using the batch exchange method (Cerri et al. 2002). We subjected 1.0 g zeolite samples in Nalgene™ tubes with 35 mL of 1M NH<sub>4</sub>Cl solution to continuous stirring under a constant temperature of about 60°C. Every 2 h, the exhausted solution was separated from the solid by centrifugation and replaced with the same volume of a fresh one. At the end of the runs, the concentrations of cations released from zeolites, analyzed by inductively coupled plasma optical emission spectrometry (ICP-OES, using a Perkin Elmer Optima 2100DV apparatus), allow for the estimation of the CEC, in mEq/g. Usually, ten repetitions of the treatment were required to attain a < 0.1 mg/L concentration of cations.

The phillipsite sample was then used for equilibrium studies of the exchange reaction  $2\text{Na}^+ \rightleftharpoons \text{Cu}^{2+}$ . The sample was previously exchanged in its monocationic form (Na) following a procedure similar to the one described to obtain the cation exchange capacity. The procedure aims at obtaining a concentration of the outgoing cations (*e.g.*, K<sup>+</sup>, Ca<sup>2+</sup>, Mg<sup>2+</sup>), estimated through ICP-OES analysis, lower than 1 mg/L. The obtained mono-cationic form was then washed and dried overnight.

The sodium-form of the phillipsite sample was allowed to react at 25°C in 25 mL sealed Nalgene™ test tubes with 10 mL solutions, containing varying amounts of Na<sup>+</sup> and Cu<sup>2+</sup> at 0.1 total normality, prepared starting from the relevant reagent-grade Carlo Erba RPE nitrates. Reversibility ion exchange tests were performed following the recommendations of Fletcher and Townsend (Fletcher et al. 1981). The solid-to-liquid ratio was varied between 1/100 and 1/500. The reaction

time was fixed at 3 d, which was beforehand proved to be sufficient to attain equilibrium.  $\text{Cu}^{2+}$  and  $\text{Na}^+$  concentrations in the liquid phase were measured by ICP-OES, whereas the concentration of the exchangeable cations in solids was calculated by mass balance.

In order to prepare a copper form of the selected zeolite, a sample of Na-exchanged zeolite was contacted with 0.1N  $\text{Cu}^{2+}$  solution -  $\text{Cu}(\text{NO}_3)_2$  Carlo Erba RPE - for a week, replacing the exhausted solution with a fresh one every 12 h and analyzing the eluted by ICP-OES for Cu and Na content. Natural, Na- and Cu-exchanged forms were analyzed by (Figure 2). Interestingly, the final Cu-exchanged polycrystalline material was green-bluish, as shown in Figure 3 (deposited).

The polycrystalline material of the Cu-exchanged form was characterized by synchrotron X-ray powder diffraction at the ID09A beamline at the European Synchrotron Radiation Facility (ESRF), Grenoble (France). Data were collected in transmission mode using monochromatic beam of 0.4145 Å with a MAR555 flat panel detector. Data reduction was performed with the FIT2D software (Hammersley et al. 1996). The diffraction pattern was successfully indexed with the unit-cell parameters of phillipsite reported by Gatta et al. (2009, 2010); a few un-indexed weak Bragg peaks are due to a minor fraction of chabazite. In order to describe the extra-framework configuration of the Cu-phillipsite, a structure refinement was performed by Rietveld method (Rietveld 1969) using the GSAS package (Larson and Von Dreele 1994), starting from the structure model of phillipsite reported by Gatta et al. (2009, 2010). Geometrical soft-restraints on T-O distances were applied on the basis of the experimental findings of Gatta et al. (2009), with an estimated standard deviation of  $\pm 0.08$  Å. The whole diffraction pattern was fitted using a pseudo-Voigt profile function (Thomson et al. 1987) and the background curve was modeled with a Chebyshev polynomial (20 terms). The first cycles of refinement were conducted without any extra-framework site. The channel population was then allocated on the basis of the maxima in the difference-Fourier map of the electron density. The best figures of merit were obtained for a structure model with three independent cation sites (modeled with a mixed Na+Cu scattering curve) and five independent  $\text{H}_2\text{O}$  sites with partial site occupancy (Table 1). The weight of the soft

constraints was decreased in the last cycles of refinement, to a final value of  $F=100$  (as implemented in GSAS). When convergence was achieved (Figure 4), no significant correlation was observed in the variance-covariance matrix and no significant residuals were found in the difference-Fourier map. The broad diffraction peaks and the anomalously high background suggest a low crystallinity of the material (dominant phillipsite and minor chabazite) coupled with a simultaneous presence of an amorphous fraction.

Cu-phillipsite was also investigated by transmission electron microscopy (TEM). The sample was prepared by gentle grinding in an agate mortar, suspension in isopropyl alcohol and deposition on a holey carbon coated grid. TEM observations were carried out on a field emission gun FEI Tecnai F20 super twin electron microscope, equipped with Gatan Slow Scan CCD 794 and operated at 200kV at the Dip. Scienze della Terra – Università degli Studi di Milano. The microscope is equipped with an EDS detector, for qualitative and semi-quantitative chemical analyses.

## Results and discussion

The exchange isotherm of the pair  $\text{Na}^+/\text{Cu}^{2+}$  on phillipsite, reported in Figure 5, lies below the diagonal over the whole composition range, demonstrating a substantial selectivity lack of phillipsite for  $\text{Cu}^{2+}$ . Moreover, it seems that the total cation exchange capacity of the sample is not available for the exchange reaction. Actually, the exhaustive procedure of exchange gave rise to a final Cu equivalent fraction in zeolite of  $\sim 0.70$ . The isotherm also displays an evident hysteresis loop inasmuch as direct ( $2\text{Na}^+ \rightarrow \text{Cu}^{2+}$ ) and back ( $\text{Cu}^{2+} \rightarrow 2\text{Na}^+$ ) exchange runs gave results that could be fitted by two distinct curves over the whole composition range.

The poor selectivity exhibited by phillipsite for the divalent cation is well explained according to the Eisenman's theory of cation exchange selectivity (Eisenman 1962; Sherry 1969), which predicts that zeolites having medium-high Si/Al ratios prefer in uni-divalent exchanges monovalent cations or divalent cations with low energy of hydration. The obtained results are



confirmed by previous literature data. Colella et al. (1998), by analyzing the  $2\text{Na}^+/\text{Cu}^{2+}$  exchange process on a pure phillipsite, reported a quite low and incomplete selectivity of the zeolite towards the incoming cation, as well as a hysteresis between the direct and back exchange, although less marked if compared to the one of this study. This behavior of the exchange process was tentatively explained by Colella et al. (1998) as a consequence of a difficult access of the incoming cation to the extra-framework sites, mostly due to the large size of its hydrated form ( $\text{Cu}^{2+}$  hydration energy equal to  $-2100 \text{ kJ/mol}$  vs.  $-405 \text{ kJ/mol}$  for  $\text{Na}^+$ ). The lack of reversibility evidenced by the hysteresis was explained as follows: the difficult access of  $\text{Cu}^{2+}$  in the zeolite structure leads to a distortion of the channels that, in some instances, hinders the counter exchange with  $\text{Na}^+$ . This aspect could find a validation also if one considers that the exchange is occurring between a mono- and a bivalent cation. Colella et al. (1998) concluded that an unambiguous explanation of the copper exclusion requires a more detailed structural analysis. Such an attempt was carried out in the present investigation. The implementation of more advanced techniques allowed shedding new light on this aspect by means of Rietveld structure refinement and TEM investigation, which is usually considered not suitable to examine labile phases such as zeolites. Such structural analysis seems to demonstrate that the supposed exchange process  $2\text{Na}^+ \rightarrow \text{Cu}^{2+}$  actually does not represent the main reaction mechanism, at least under the aforementioned operating conditions.

The quality of the X-ray synchrotron structure refinement is severely affected by the low crystallinity of the material, but the refined model suggests that a small, but significant, fraction of Cu likely shares with Na the three independent cation sites (*i.e.*, A1, A2 and A3; Figure 6, Table 1). In particular, the site electron contents of A1, A2 and A3 (*i.e.*,  $\Sigma e^-(\text{A1}) = 14.2 e^-$ ,  $\Sigma e^-(\text{A2}) = 3.7 e^-$ ,  $\Sigma e^-(\text{A3}) = 17.5 e^-$ ) reflect the higher presence of Cu at A1 and A3 sites. The presence of Cu at the A2 site cannot be unambiguously inferred. A1 and A2 site coordinates are in line with the I and II sites, respectively, reported by Gualtieri et al. (2002) in their comparative study on ion-exchanged phillipsites. The extra-framework population of the Cu-phillipsite is represented by three cation sites and five independent  $\text{H}_2\text{O}$  sites (*i.e.*, W1, W2, W3, W4, W5; Figure 6, Table 1). Cation and

H<sub>2</sub>O sites show partial site occupancies and several of them are mutually exclusive, making the description of the coordination scheme ambiguous. The significantly high displacement parameters of the cation sites, modelled isotropically here, reflect a multi-elemental site population, resulting in a positional disorder. The coordination spheres of the A1, A2 and A3 sites are here described assuming the longest bond distances of ~3.2 Å. The coordination polyhedron of the A1 site is represented by five oxygen atoms belonging to the tetrahedral framework (*i.e.*, O3 x 2, O5 x 2, and O8; Table 1) and three H<sub>2</sub>O molecules (*i.e.*, W1 and W5 x 2; Table 1), whereas that of A3 is represented by two oxygen atoms of the tetrahedral framework (*i.e.*, O2 x 2; Table 1) and five H<sub>2</sub>O molecules (*i.e.*, W1, W2 x 2, and W3 x 2; Table 1). More difficult is the description of the scarcely occupied A2 site, with two oxygen atoms of the framework (*i.e.*, O6 and O7; Table 1) and at least three H<sub>2</sub>O molecules (*i.e.*, W2, W4 and W5; Table 1), forming a highly distorted coordination polyhedron. Na and Cu can have significantly different coordination environments in zeolites. On the basis of EXAFS spectra, Cu was found to have a 2- or 3-fold coordination in some Cu-exchanged zeolites (*e.g.*, in Cu-Y, Cu-ZSM-5 or Cu-MOR), with Cu–O bond distance of about 2 Å (Zhang et al. 2007). Where Na and Cu populate the same site, the coordination shell is expected to be different. For example, Cu at the site A1 might simply bind to two W5 at ~2.03 Å (Table 1). Several cation-H<sub>2</sub>O or H<sub>2</sub>O-H<sub>2</sub>O sites are mutually exclusive (as deducible by the bond distances *e.g.* A2-W2 = 1.00(7) Å, A2-W3 = 1.7(7) Å, A2-W3 = 1.4(2) Å, A2- W4 = 1.05(7) Å, W2-W2 = 1.2(1) Å, W2-W3 = 1.0(1) Å, W2-W3 = 0.9(1) Å, W3-W3 = 0.2(3) Å, or W5-W5 = 1.11(9) Å, Table 1). As previously observed for natural phillipsites (*e.g.*, Rinaldi et al. 1974; Gatta et al. 2009, 2010), the tetrahedral bond distances reflect a highly disordered Si/Al-distribution between the tetrahedral sites (Table 1).

The TEM investigation shows that the sample treated with Cu contains idiomorphic crystals of phillipsite (Figures 7 and 8) immersed in a significant fraction of amorphous material. Sub-spherical nano-clusters of crystalline species (as shown by the high-resolution images), with an average size of 5 nm, lie on the surfaces of zeolite crystals or dispersed in the amorphous fraction

(Figure 9). The electron diffraction pattern of the nano-aggregates shows inter-planar distances consistent with those of CuO (tenorite-like structure,  $a \sim 4.65$ ,  $b \sim 3.42$ ,  $c \sim 5.13$ ,  $\beta \sim 99.47^\circ$ , space group:  $C2/c$ ) and Cu(OH)<sub>2</sub> (spertiniite-like structure,  $a \sim 2.93$ ,  $b \sim 10.54$ ,  $c \sim 5.23$ , space group:  $Cmc2_1$ ) (Figure 10). A few crystals of chabazite have also been found (Figure 7), as previously shown by X-ray diffraction.

The combination of X-ray powder diffraction, with a Rietveld structure refinement, along with the TEM investigation provided the key to understand: *a*) the poor selectivity exhibited by phillipsite for the divalent cations, and in particular for Cu, as observed by Colella et al. (1998); *b*) the colour of the Cu-exchanged sample, which appears to be governed by the presence of Cu-oxyhydroxides. The X-ray structure refinement of Cu-exchanged phillipsites does not show a high Cu/Na fraction at the extra-framework sites; this suggests that Cu is mainly concentrated in different species (crystalline or amorphous) of the sample, and not only in phillipsite. The TEM experimental findings show that Cu is also concentrated in sub-spherical CuO (tenorite-like) and Cu(OH)<sub>2</sub> (spertiniite-like) nano-clusters dispersed in the amorphous phase or on the crystal surfaces. As expected, no Cu-bearing nano-compounds were observed in the X-ray diffraction patterns. The presence of nano-aggregates on the crystal surface of clinoptilolite, in response to cation exchange experiments, was reported in a recent study on the sorption of lead by natural and Fe(III)-modified clinoptilolite-rich sample (Kragović et al. 2013). The X-ray powder diffraction patterns did not show any evidence of crystalline Fe-bearing phases after an Fe(III)-treatment, and the EDS analyses showed that: 1) the amount of Fe and Pb in idiomorphic crystals of clinoptilolite was negligible (*i.e.* below the EDS detection limit), and so Fe and Pb were not concentrated in the zeolite structure (*i.e.* as extra-framework population); 2) Fe and Pb were mainly concentrated in the amorphous fraction. Under the TEM, Kragović et al. (2013) observed the presence of sub-spherical and amorphous Fe-Pb-bearing nano-clusters dispersed on the surface of the clinoptilolite crystals. Those experimental findings explained the absence of Fe- or Pb-bearing oxides/hydroxides in the X-ray diffraction patterns of the lead-saturated natural and Fe(III)-modified samples.

The results obtained in this study on phillipsite can be interpreted by means of a double mechanism:

(1) In the first steps, the main process is an ion exchange interaction between solution and phillipsite samples (kinetic aspect dominant), enabling the access of a copper ions slice to the extra-framework sites of the zeolite. This mechanism is facing difficulties due to the uni-divalent exchange, in accordance with Eisenman's (1962) and Sherry's (1969) theory.

(2) The interaction between the zeolite, in its sodium form, and the solution, having a starting measured pH of  $\sim 3.5$ , causes a sudden increase of the solution pH to alkaline values (pH = 8-9). This increase, related to the low solubility of the copper hydroxide ( $\text{Cu}(\text{OH})_2$  solubility =  $4.8 \cdot 10^{-20}$ ), leads to a precipitate formation, making this the prevailing mechanism. Lastly, a partial transition from hydroxide to copper oxide occurs during the subsequent filtration step (solid-phase separation from liquid and solid-phase drying), thus providing a further possible explanation for the colour change of the polycrystalline sample.

The experimental findings of this study and those reported by Kragović et al. (2013) force us to reconsider the role played by surface phenomena on zeolite crystals and by the (X-ray) amorphous fraction when transition elements are used. The results of the present study on phillipsite show under a new perspective all processes, defined as ion exchange, which involve natural zeolitized materials and cations of different nature for which the equilibrium runs behaviour shows unusual phenomena, *e.g.* hysteresis of exchange isotherms as indication of a partial reversibility of the exchange reaction. The partial reversibility might be likely controlled by the precipitation mechanisms of new phases on the surfaces of zeolitised material. In the case of natural zeolites, such "anomalies" occur when cations, at least divalent and characterized by high hydration energy, are involved in the exchange reactions. It will be, therefore, necessary to better investigate the mechanisms active in these cases, evaluating the operating parameters of the ion exchange processes, such as the solid-liquid ratio, starting solution concentration, or "scale up" effect of the equilibrium runs.

## **Acknowledgements**

GDG and NR acknowledge the Italian Ministry of Education, MIUR-Project: “Futuro in Ricerca 2012 - ImPACT- RBFR12CLQD”. The European Synchrotron Radiation Facility, Grenoble, France, is thanked for the allocation of beam time. The authors thank Marco Merlini for the collection of the synchrotron X-ray diffraction data, and Vincenzo Monetti for the exchange procedures. Two anonymous reviewers are thanked.

## References

- Alberti A (1978) Differenze di chimismo tra zeoliti idrotermali e sedimentarie. *Rend Soc Ital Mineral Petrogr* 34:471–484.
- Černý P (1964) The phillipsite-wellsite-harmotome symmetry: orthorhombic or monoclinic? *Neues Jahrbuch Mineral Monatsh* 5:129–134.
- Cerri G, Langella A, Pansini M, Cappelletti P (2002) Methods of determining cation exchange capacities for clinoptilolite-rich rocks of the Logudoro region in northern Sardinia, Italy. *Clays Clay Min* 50:127–135.
- Colella C, de' Gennaro M, Langella A, Pansini M (1998) Evaluation of natural phillipsite and chabazite as cation exchangers for copper and zinc. *Separation Science and Technology* 33:467–481.
- Coombs DS, Alberti A, Armbruster T, Artioli G, Colella C, Grice JD, Galli E, Liebau F, Minato H, Nickel EH, Passaglia E, Peacor DR, Quartieri S, Rinaldi R, Ross M, Sheppard RA, Tillmans E, Vezzalini G (1997) Recommended Nomenclature for Zeolite Minerals: Report of the Subcommittee on Zeolite of the International Mineralogical Association Commission on New Minerals and Mineral Names. *Can Mineral* 35:1571–1606.
- de' Gennaro M, Cappelletti P, Langella A, Perrotta A, Scarpati C (2000) Genesis of zeolites in the Neapolitan Yellow Tuff: geological, volcanological and mineralogical evidences. *Contrib Mineral Petrol* 139:17–35.
- de' Gennaro M, Franco E, Langella A, Mirra P, Morra V (1982) Le zeoliti delle piroclastiti dei Monti Ernici. La phillipsite dei peperini. *Acta Naturalia de l'Ateneo Parmense* 18:163–176.
- de' Gennaro, M., Langella, A., Cappelletti, P., Colella, C. (1999) Hydrothermal conversion of trachytic glass to zeolite. 3. Monocationic model glasses. *Clays Clay Min* 47:348–357.
- de' Gennaro M, Petrosino P, Conte MT, Munno R, Colella C (1990) Zeolite chemistry and distribution in a Neapolitan yellow tuff deposit. *Eur J Mineral* 2:779–786.

Eisenman G (1962) Cation selective glass electrodes and their mode of operation. *Biophys J* 2:259–323.

Fletcher P, Townsend RP (1981) Transition metal ion exchange in zeolites. Part 4. –Exchange of hydrated and amminated silver in sodium X and Y zeolites and mordenite. *J Chem Soc Faraday Trans 77*: 497–509.

Galli E, Loschi-Ghittoni AG (1972) The crystal chemistry of phillipsites. *Am Mineral* 57:1125–1145.

Gatta GD, Cappelletti P, Rotiroti N, Slebodnick C, Rinaldi R (2009) New insights into the crystal structure and crystal chemistry of the zeolite phillipsite. *Am Mineral* 94:190–199.

Gatta GD, Cappelletti P, Langella A (2010) Crystal-chemistry of phillipsites from the Neapolitan Yellow Tuff. *Eur J Mineral* 22:779–786.

Gottardi G, Galli E (1985) *Natural Zeolites*, Springer-Verlag, Berlin, Germany, 409 p.

Gualtieri AF (2000) Study of  $\text{NH}_4^+$  in the zeolite phillipsite by combined synchrotron powder diffraction and IR spectroscopy. *Acta Crystallogr B* 56:584–593.

Gualtieri A.F., Caputo D., Colella C. (1999a) Ion-exchange selectivity of phillipsite for  $\text{Cs}^+$ : a structural investigation using the Rietveld method. *Micropor Mesopor Mat* 32:319–329.

Gualtieri A.F., Passaglia E., Galli E., Viani A. (1999b) Rietveld structure refinement of Sr-exchanged phillipsites. *Micropor Mesopor Mat* 31:33–43.

Gualtieri A.F., Passaglia E., Galli E. (2000) Rietveld structure refinement of natural and Na-, K-, Ca-, and Ba-exchanged phillipsites. In C. Colella and F.A. Mumpton, Eds., *Natural zeolites for the third millennium*. De Frede, Naples, Italy, p. 93–110.

Gualtieri AF, Passaglia E, Galli E (2002) Ion exchange selectivity of phillipsite. *Studies in Surface Science and Catalysis* 142, R. Aiello, G. Giordano and F. Teast, Eds., Elsevier Science, 1705–1711.

Hammersley AP, Svensson SO, Hanfland M, Fitch AN, Häusermann D (1996) Two-dimensional detector software: from real detector to idealised image or two-theta scan. *High Pressure Res* 14:35–248.

Insinga D, Calvert AT, Lanphere MA, Morra V, Perrotta A, Sacchi M, Scarpati C, Saburomaru J, Fedele L (2006) The Late-Holocene evolution of the Miseno area (south-western Campi Flegrei) as inferred by stratigraphy, petrochemistry and  $^{40}\text{Ar}/^{39}\text{Ar}$  geochronology. In B. De Vivo, Ed., *Volcanism in the Campania Plain: Vesuvius, Campi Flegrei and Ignimbrites*. *Developments in Volcanology, Series 9*, Elsevier, p. 97–125.

Kragović M, Daković A, Sekulić Ž, Trgo M, Ugrina M, Perić J, Gatta GD (2012) Removal of lead from aqueous solutions by using the natural and Fe(III)-modified zeolite. *Appl Surface Science* 258:3667– 3673.

Langella A, Cappelletti P, de’Gennaro R (2001) Zeolites in closed hydrologic systems. In D.L. Bish and D.W. Ming, Eds., *Natural zeolites: occurrence, properties, application*, Vol. 45, p. 235–260. *Reviews in Mineralogy and Geochemistry*, Mineralogical Society of America and Geochemical Society, Washington, U.S.A.

Larson AC, Von Dreele RB (1994): *General Structure Analysis System (GSAS)*, Los Alamos National Laboratory Report LAUR 86-748.

Ming DW, Mumpton FA (Eds.) (1995) *Natural Zeolites '93: Occurrence, Properties, Use*. International Committee on Natural Zeolites, Brockport, New York, 622 p.

Passaglia E, Sheppard RA (2001) The crystal chemistry of zeolites. In D.L. Bish and D.W. Ming, Eds., *Natural zeolites: occurrence, properties, application*, Vol. 45, p. 69–116. *Reviews in Mineralogy and Geochemistry*, Mineralogical Society of America and Geochemical Society, Washington, U.S.A.

Passaglia E, Vezzalini G (1985) Crystal chemistry of diagenetic zeolites in volcanoclastic deposits of Italy. *Contrib Miner Petrol* 90:190–198.

Rietveld HM (1969) A profile refinement method for nuclear and magnetic structures. *J Appl*



Cryst 2:65–71.

Rinaldi R, Pluth JL, Smith JV (1974) Zeolites of the phillipsite family. Refinement of the crystal structures of phillipsite and harmotome. *Acta Crystallogr B*30:2426–2433.

Rinaldi R, Smith JV, Jung G (1975) Chemistry and paragenesis of faujasite, phillipsite and offretite from Sasbach, Kaiserstuhl, Germany. *Neues Jahrbuch Mineral Monatsh* 10:433–443.

Sheppard RA, Hay RL (2001) Formation of zeolites in open hydrologic systems. In D.L. Bish and D.W. Ming, Eds., *Natural zeolites: occurrence, properties, application*, Vol. 45, p. 261–275. *Reviews in Mineralogy and Geochemistry*, Mineralogical Society of America and Geochemical Society, Washington, U.S.A.

Sherry HS (1969) The Ion-Exchange Properties of Zeolites. In J.A. Marinsky, Ed., *Ion Exchange: A Series of Advances*, Vol. 2, p. 89–133. Marcel Dekker, New York.

Thompson P, Cox DE, Hastings JB (1987) Rietveld refinement of Debye-Scherrer synchrotron X-ray data from Al<sub>2</sub>O<sub>3</sub>. *J Appl Cryst* 20:79–83.

Tsitsishvili GV, Andronikashvili TG, Kirov GN, Filizova LD (1992) *Natural Zeolites*. Ellis Horwood Ltd., England, 295 p.

Zhang Y, Briggs DN, de Smit E, Bell AT (2007) Effects of zeolite structure and composition on the synthesis of dimethyl carbonate by oxidative carbonylation of methanol on Cu-exchanged Y, ZSM-5, and Mordenite. *J Catalysis* 251:443–452.

## Captions

### Tables

Table 1. Data pertaining to the structure refinement parameters, atomic positions, site occupancy factors (*s.o.f.*), isotropic displacement parameters ( $\text{\AA}^2$ ) and bond-distances ( $\text{\AA}$ ) of the Cu-exchanged phillipsite.

### Figures

Figure 1. Sketch map of the Campi Flegrei volcanic district (modified after Gatta et al. 2010). The sample used for the present investigation comes from an outcrop of NYT within the caldera of Campi Flegrei, namely Grotta del Sole locality (labelled “P7”).

Figure 2. X-ray powder diffraction patterns of natural PHI (red), Na-PHI (black) and Cu-PHI (blue). The only well-visible Bragg peak of the minor chabazite is that at the  $2\theta \sim 9.4^\circ$ , expected to be the most intensive one (see text for details).

Figure 3 (Deposited). Macroscopic picture of Na-PHI (*left side*) and Cu-PHI (*right side*) samples.

Figure 4. Experimental (crosses) and calculated (solid line) diffraction patterns of Cu-exchanged phillipsite. Calculated peak positions and difference plots are shown at the bottom of the pattern.

Figure 5. Isotherm at  $25^\circ\text{C}$  for the exchange of Cu into Na-phillipsite at 0.1 total normality. Circles = forward reactions; triangles = reversals.

Figure 6. Two views of the crystal structure of the Cu-phillipsite based on the present Rietveld structure refinement.

Figure 7. Cu-treated sample: Idiomorphic crystals of phillipsite immersed in an amorphous fraction (visible in the bottom-left corner).

Figure 8. TEM diffraction pattern of a single crystal of phillipsite (randomly oriented, *left*) and chabazite (down the pseudo-3fold axis, *right*) found in the Cu-treated sample.

Figure 9. (*Left*) Sub-spherical nano-clusters of CuO and Cu(OH)<sub>2</sub> dispersed in the amorphous fraction. (*Right*) TEM high-resolution image showing the crystalline nature of nano-clusters of CuO and Cu(OH)<sub>2</sub>.

Figure 10. Diffraction pattern of the nano-clusters. The inter-planar distances are compatible with those of CuO (tenorite-like,  $a \sim 4.65$ ,  $b \sim 3.42$ ,  $c \sim 5.13$ ,  $\beta \sim 99.47^\circ$ , space group:  $C2/c$ ) and Cu(OH)<sub>2</sub> (spertiniite-like,  $a \sim 2.93$ ,  $b \sim 10.54$ ,  $c \sim 5.23$ , space group:  $Cmc2_1$ )

Table 1. Data pertaining to the structure refinement parameters, atomic positions, site occupancy factors (*s.o.f.*), isotropic displacement parameters ( $\text{\AA}^2$ ) and bond-distances ( $\text{\AA}$ ) of the Cu-exchanged phillipsite.

Site (Wyck.)	x	y	z	<i>s.o.f.</i> ( <i>e</i> )	$U_{\text{iso}}$				
T1 (4 <i>f</i> )	0.737(2)	0.013(2)	0.278(3)	14	0.0232(8)	T1-O2	1.641(2)	A1-W5 (x2)	2.03(5)
T2 (4 <i>f</i> )	0.431(2)	0.141(1)	0.028(3)	14	0.0232(8)	T1-O3	1.641(2)	A1-O8	2.94(8)
T3 (4 <i>f</i> )	0.057(2)	0.008(2)	0.285(3)	14	0.0232(8)	T1-O5	1.640(3)	A1-W1	2.71(6)
T4 (4 <i>f</i> )	0.111(2)	0.140(1)	0.020(3)	14	0.0232(8)	T1-O7	1.641(2)	A1-O3 (x2)	3.06(5)
O1 (4 <i>f</i> )	0.093(5)	0.088(2)	0.176(4)	8	0.038(3)			A1-O5 (x2)	3.02(2)
O2 (4 <i>f</i> )	0.641(5)	0.584(2)	0.168(4)	8	0.038(3)	T2-O2	1.642(2)		
O3 (4 <i>f</i> )	0.616(3)	0.105(2)	0.192(5)	8	0.038(3)	T2-O3	1.641(3)	A2-W2	2.12(8)
O4 (4 <i>f</i> )	0.027(4)	0.905(2)	0.185(4)	8	0.038(3)	T2-O6	1.642(3)	A2-W5	2.84(8)
O5 (4 <i>f</i> )	0.894(2)	0.043(2)	0.273(3)	8	0.038(3)	T2-O8	1.642(3)	A2-O7	3.25(9)
O6 (4 <i>f</i> )	0.298(2)	0.377(2)	0.081(3)	8	0.038(3)			A2-O6	3.23(7)
O7 (4 <i>f</i> )	0.793(3)	0.489(4)	0.495(3)	8	0.038(3)	T3-O1	1.641(3)	A2-W4	3.15(7)
O8 (2 <i>e</i> )	0.517(7)	3/4	-0.019(8)	8	0.038(3)	T3-O4	1.640(2)		
O9 (2 <i>e</i> )	0.048(6)	1/4	-0.030(7)	8	0.038(3)	T3-O5	1.642(2)	A3-W1	2.14(9)
A1 (2 <i>e</i> )	0.834(5)	1/4	0.172(3)	14.2	0.072(8)	T3-O7	1.651(3)	A3-O2 (x2)	3.16(4)
A2 (4 <i>f</i> )	0.546(9)	0.355(4)	0.530(9)	3.7	0.04(2)			A3-W2 (x2)	2.68(11)
A3 (2 <i>e</i> )	1.269(4)	1/4	0.545(5)	17.5	0.22(2)	T4-O1	1.642(2)	A3-W3 (x2)	2.77(9)
W1 (2 <i>e</i> )	-0.056(7)	3/4	0.451(8)	4.8	0.026(8)	T4-O4	1.641(3)		
W2 (4 <i>f</i> )	0.504(9)	0.791(4)	0.520(6)	4.6	0.026(8)	T4-O6	1.642(3)		
W3 (4 <i>f</i> )	0.436(8)	0.742(12)	0.419(7)	3.7	0.026(8)	T4-O9	1.641(3)		
W4 (4 <i>f</i> )	0.539(9)	1.072(3)	0.539(7)	4.6	0.026(8)				
W5 (4 <i>f</i> )	0.254(6)	0.789(3)	0.096(6)	4.3	0.026(8)				
$a=9.9453(7)\text{\AA}$	$b=14.202(1)\text{\AA}$	$c=8.686(1)\text{\AA}$	$\beta=124.728(8)^\circ$	Sp. Gr.	$P2_1/m$				
<i>N.obs</i>	2229								
<i>N. variables</i>	71								
<i>Rp</i>	0.0941								
<i>wRp</i>	0.1352								
$\chi^2$	1.035								
$R(F^2)$	0.1474								
$\Delta\rho_{\text{max}}$ ( $e/\text{\AA}^3$ )	-1.3/+1.4								

*Note:* For the T1, T2, T3 and T4 sites the neutral scattering curve of silicon was used. For the A1, A2 and A3 sites, a mixed scattering curve of (50%Na+50%Cu) was adopted. The W1-5 sites were modelled with the neutral scattering curve of O. The resulting *s.o.f.* are given as electron number. One  $U_{\text{iso}}$  value for used to model all the tetrahedral sites (*i.e.*, T1-T4), one for the oxygen atoms of the tetrahedral framework (*i.e.*, O1-O9), and one for the H<sub>2</sub>O sites (*i.e.*, W1-W5), respectively. Several cation-H<sub>2</sub>O or H<sub>2</sub>O-H<sub>2</sub>O sites are mutually exclusive, as *e.g.* A2-W2 = 1.00(7)  $\text{\AA}$ , A2-W3 = 1.7(7)  $\text{\AA}$ , A2-W3 = 1.4(2)  $\text{\AA}$ , A2- W4 = 1.05(7)  $\text{\AA}$ , W2-W2 = 1.2(1)  $\text{\AA}$ , W2-W3 = 1.0(1)  $\text{\AA}$ , W2-W3 = 0.9(1)  $\text{\AA}$ , W3-W3 = 0.2(3)  $\text{\AA}$ , or W5-W5 = 1.11(9)  $\text{\AA}$ .

Figure 1. Sketch map of the Campi Flegrei volcanic district (modified after Gatta et al. 2010). The sample used for the present investigation comes from an outcrop of NYT within the caldera of Campi Flegrei, namely Grotta del Sole locality (labelled “P7”).

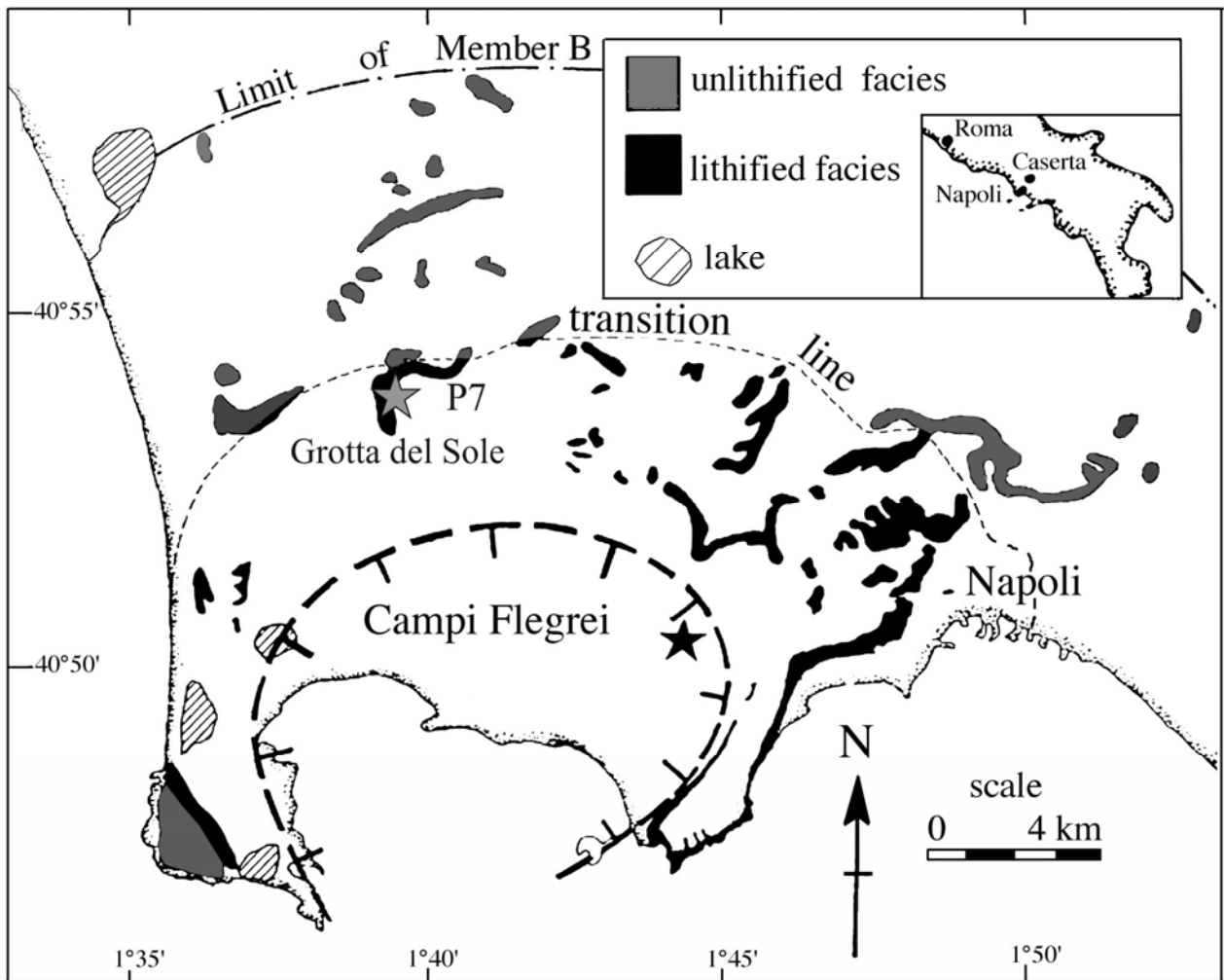


Figure 2. X-ray powder diffraction patterns of natural PHI (red), Na-PHI (black) and Cu-PHI (blue). The only well-visible Bragg peak of the minor chabazite is that at the  $2\theta \sim 9.4^\circ$ , expected to be the most intensive one (see text for details).

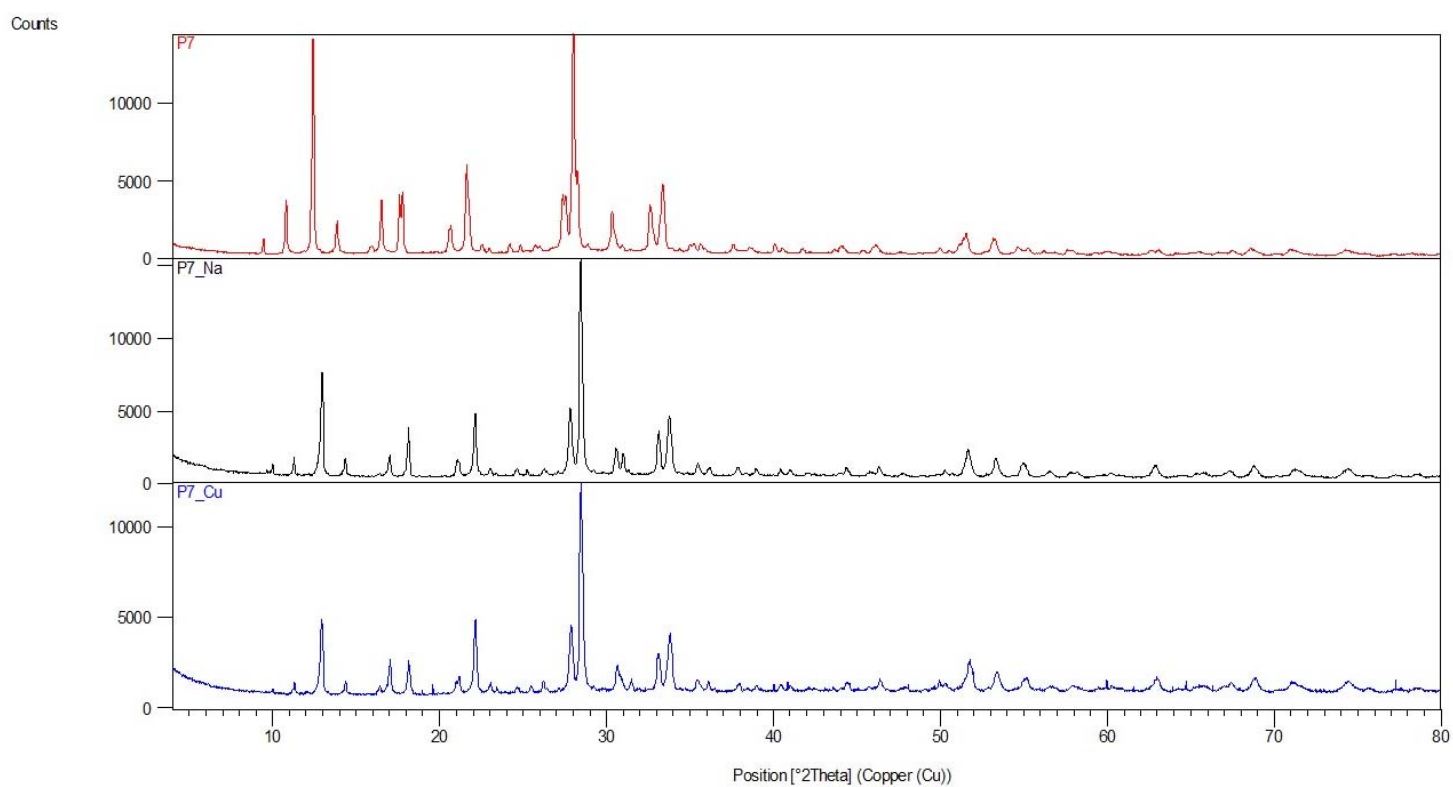


Figure 3 (Deposited). Macroscopic picture of Na-PHI (*left side*) and Cu-PHI (*right side*) samples.



Figure 4. Experimental (crosses) and calculated (solid line) diffraction patterns of the Cu-exchanged phillipsite. Calculated peak positions and difference plots are shown at the bottom of the pattern.

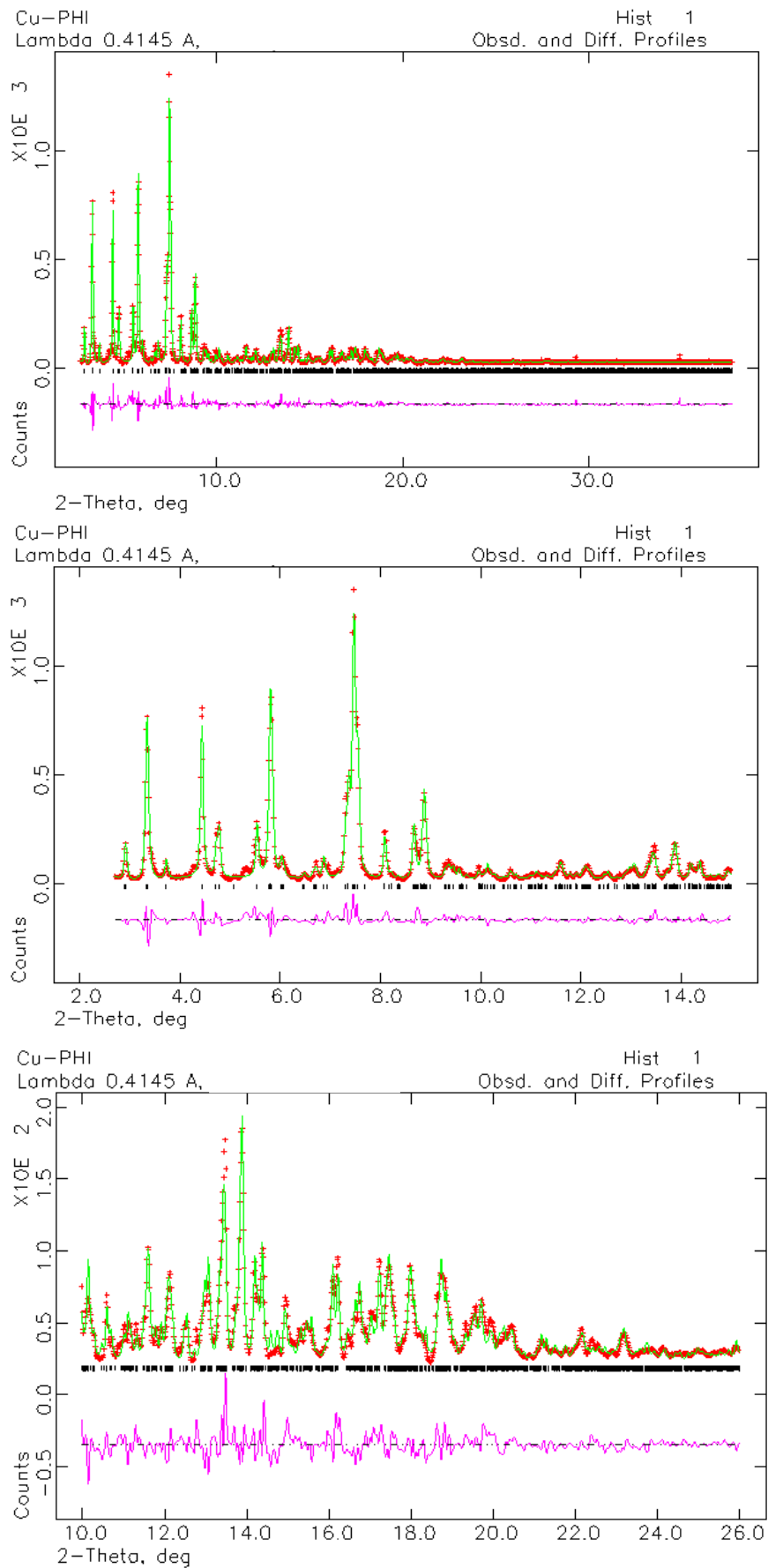




Figure 5. Isotherm at 25°C for the exchange of Cu into Na-phillipsite at 0.1 total normality. Circles = forward reactions; triangles = reversals.

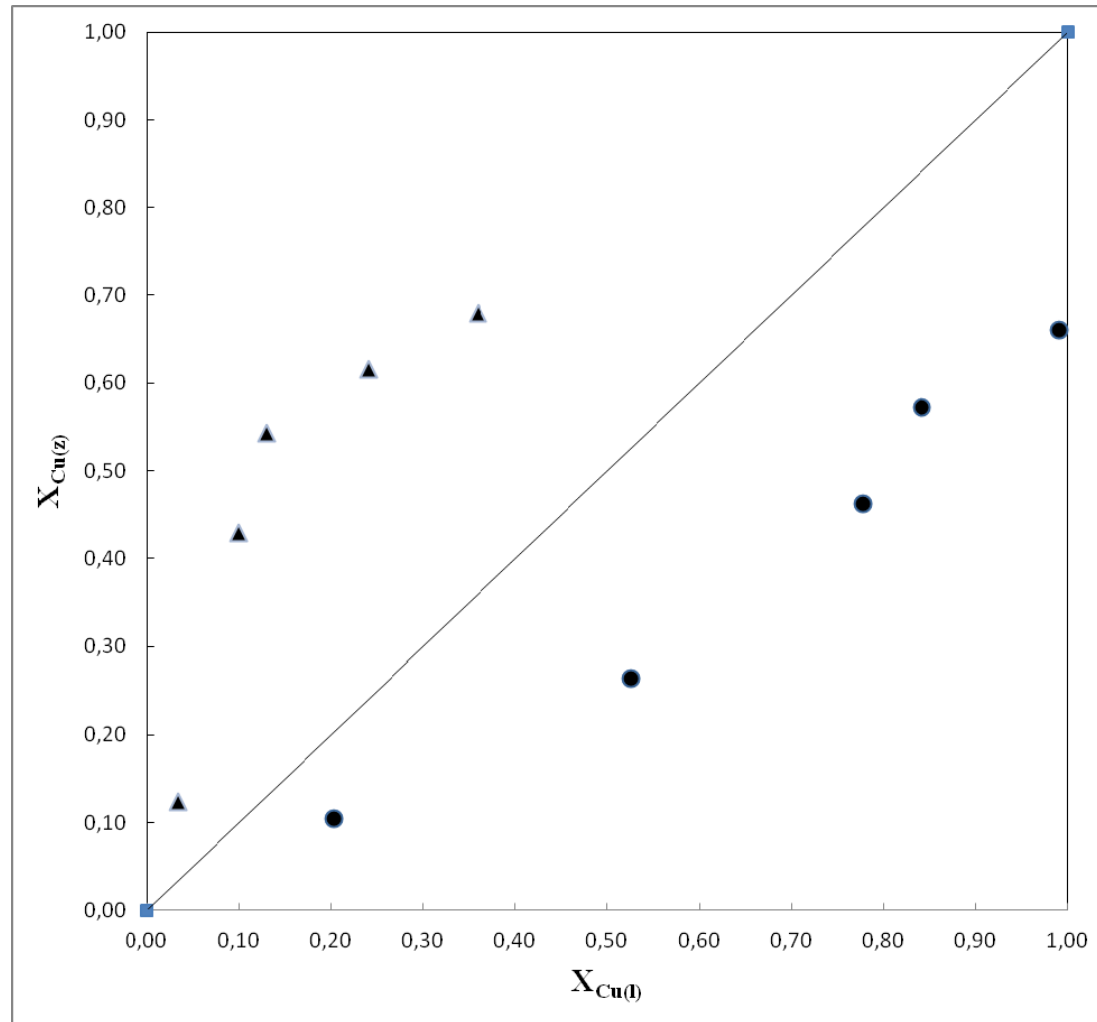


Figure 6. Two views of the crystal structure of the Cu-phillipsite based on the present Rietveld structure refinement.

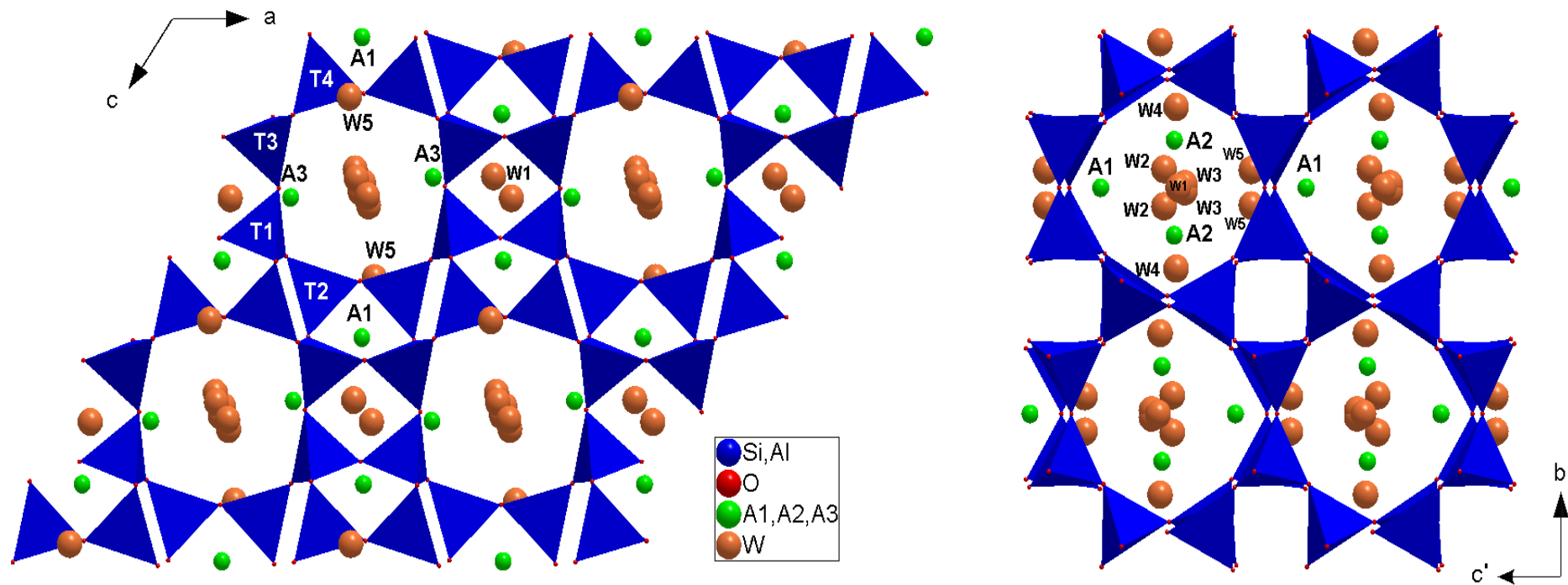


Figure 7. Cu-treated sample: idiomorphic crystals of phillipsite immersed in an amorphous fraction (visible in the bottom-left corner).

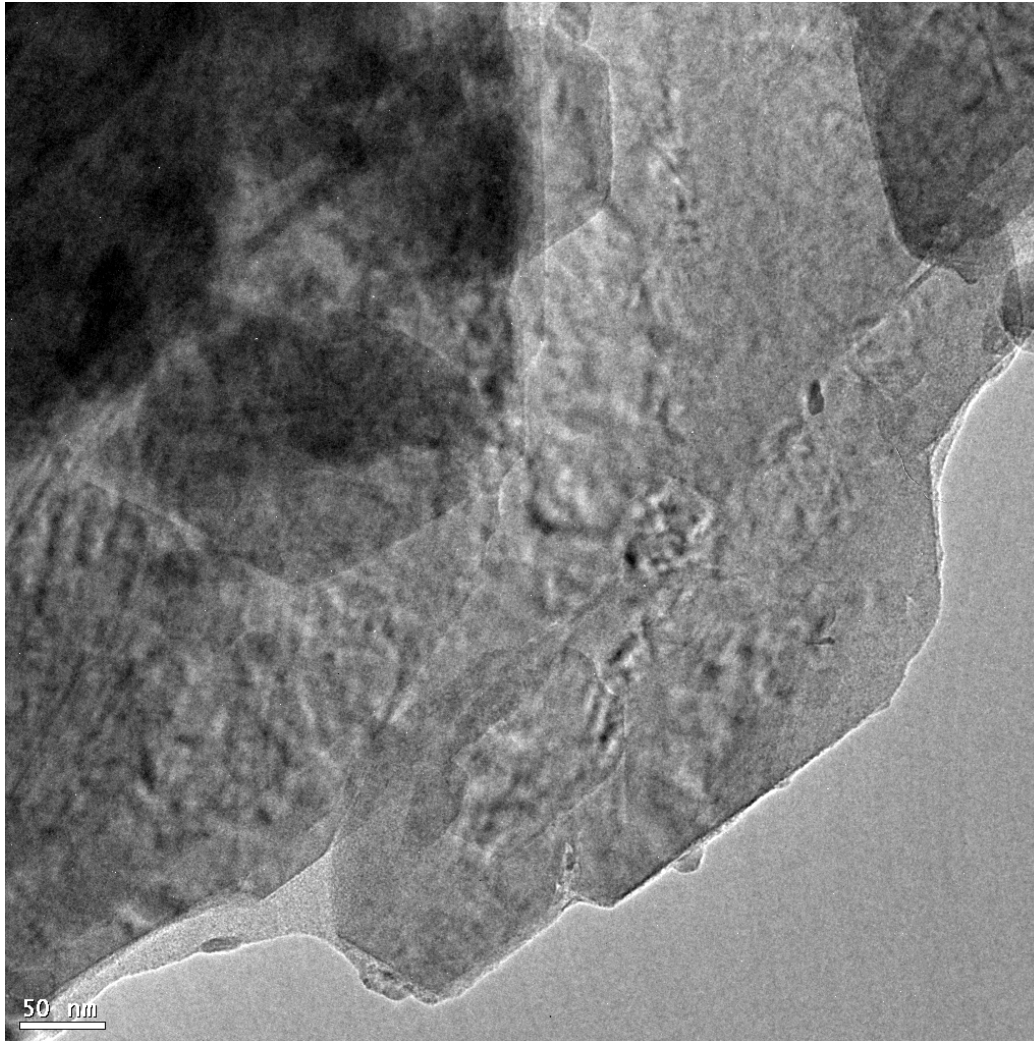


Figure 8. TEM diffraction pattern of a single crystal of phillipsite (randomly oriented, *left*) and chabazite (down the pseudo-3fold axis, *right*) found in the Cu-treated sample.

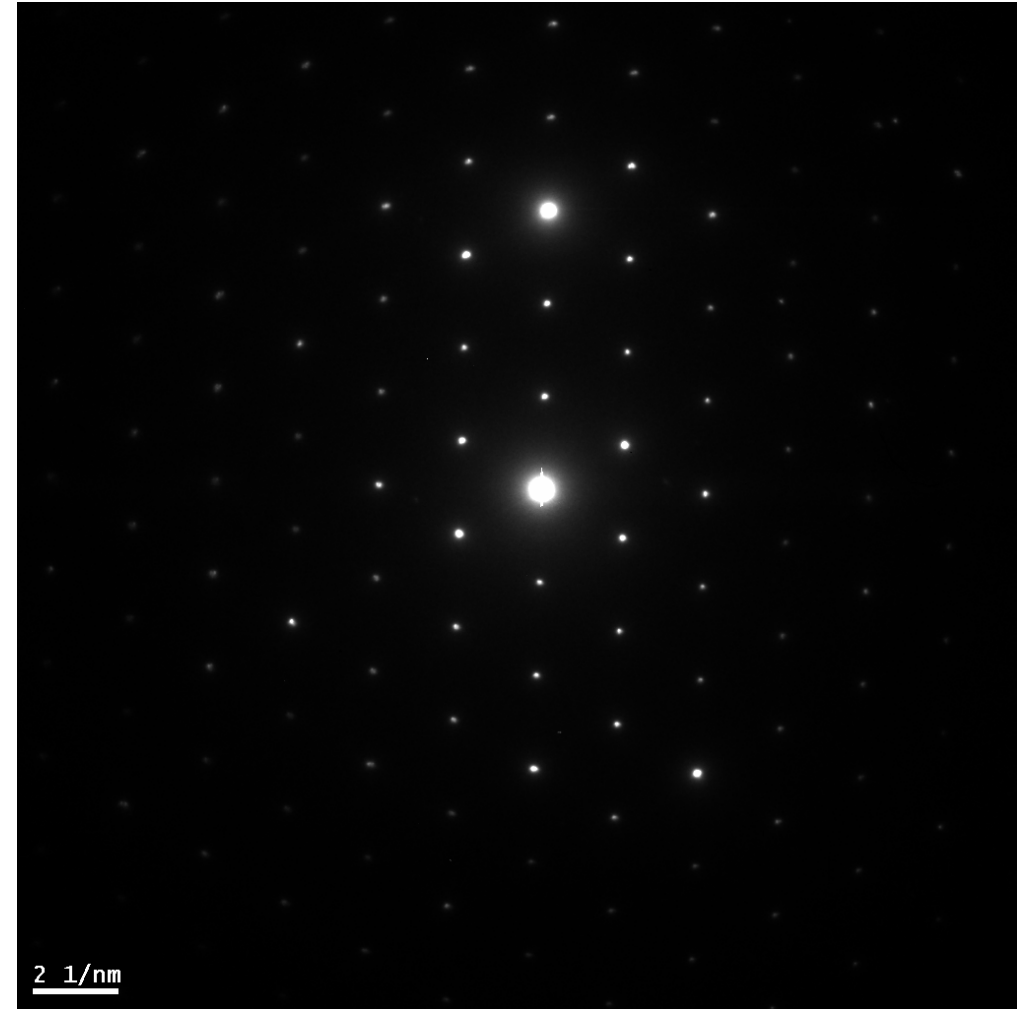
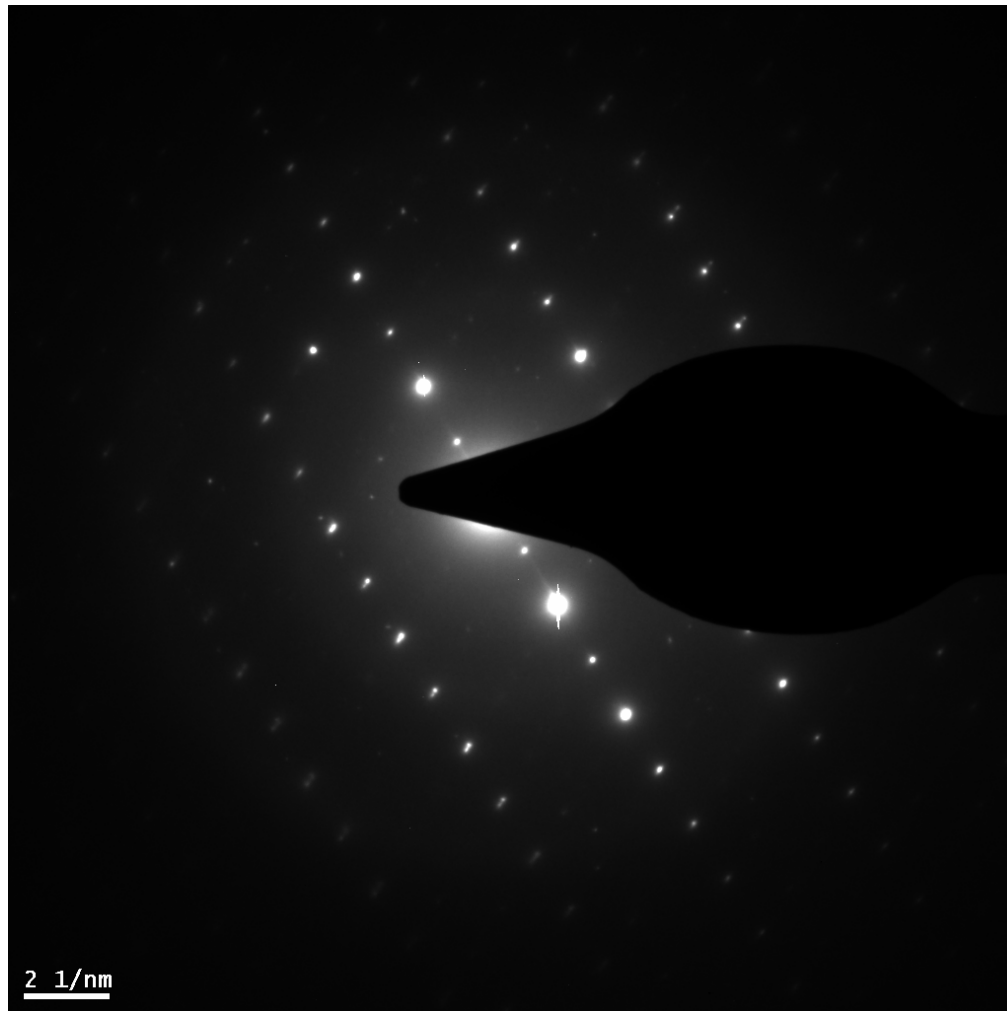


Figure 9. (Left) Sub-spherical nano-clusters of CuO and Cu(OH)<sub>2</sub> dispersed in the amorphous fraction. (Right) TEM high-resolution image showing the crystalline nature of nano-clusters of CuO and Cu(OH)<sub>2</sub>.

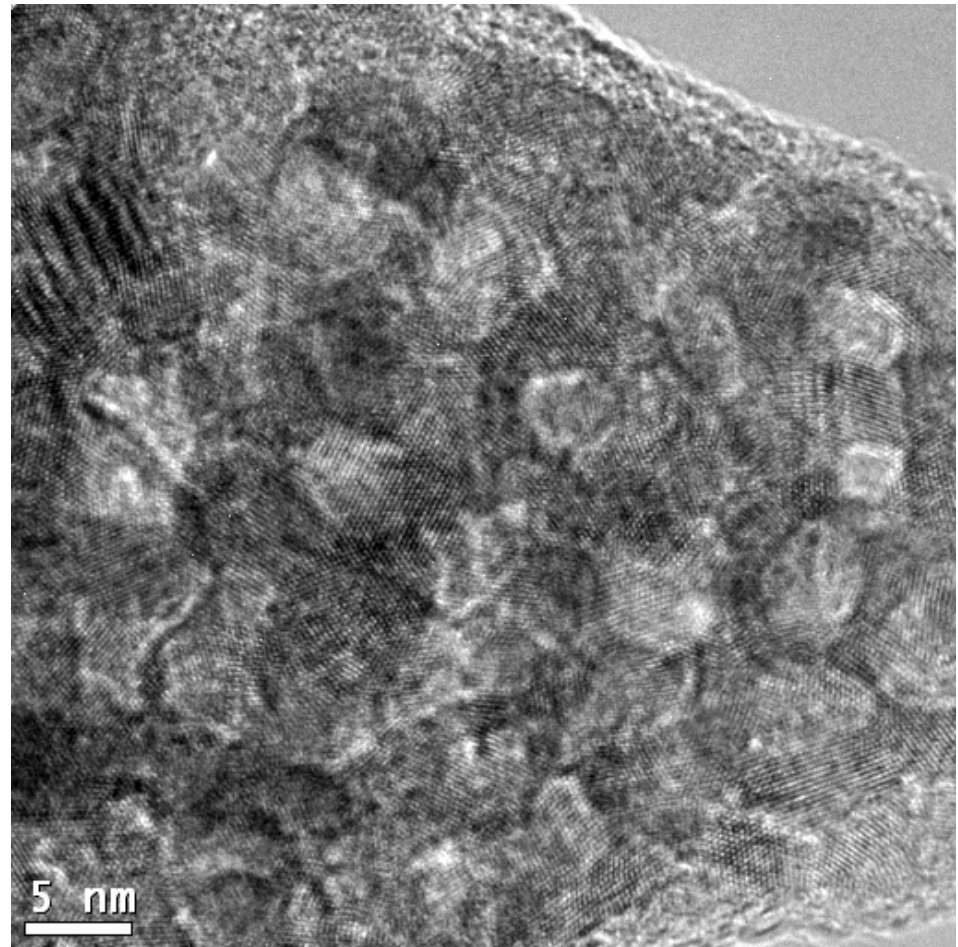
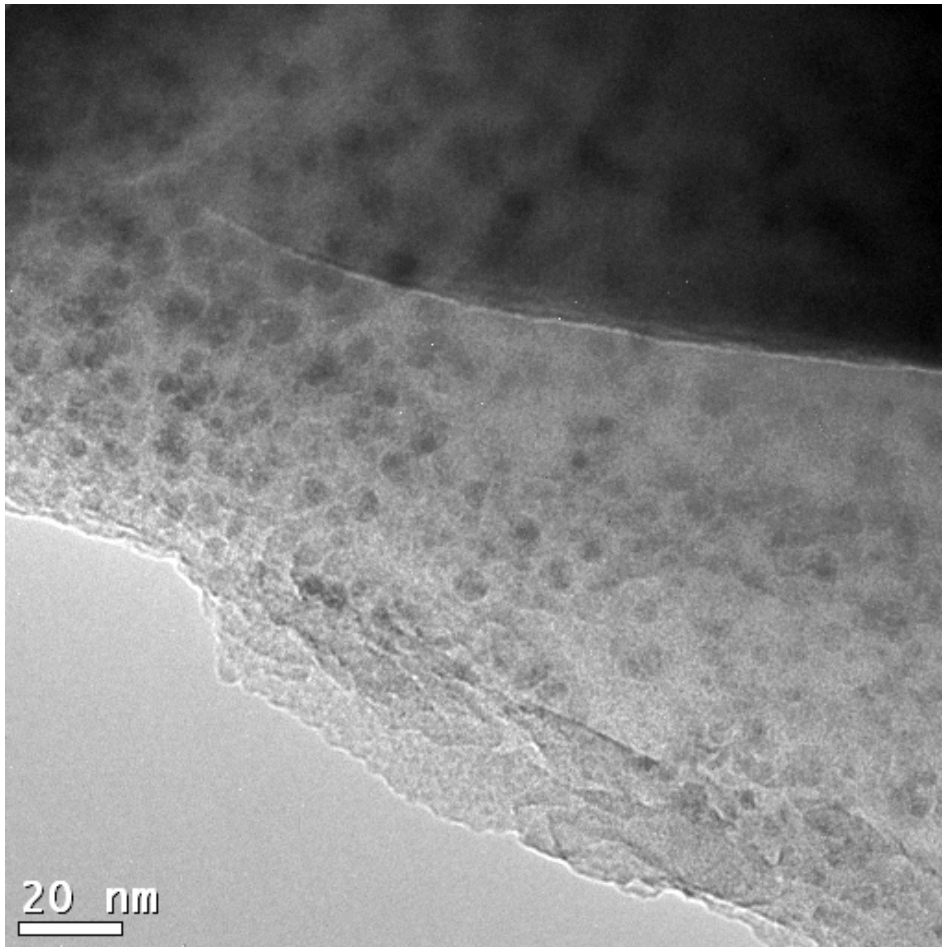


Figure 10. Diffraction pattern of the nano-clusters. The inter-planar distances are compatible with those of CuO (tenorite-like,  $a \sim 4.65$ ,  $b \sim 3.42$ ,  $c \sim 5.13$ ,  $\beta \sim 99.47^\circ$ , space group:  $C2/c$ ) and Cu(OH)<sub>2</sub> (spertiniite-like,  $a \sim 2.93$ ,  $b \sim 10.54$ ,  $c \sim 5.23$ , space group:  $Cmc2_1$ ).

